Aerospace Science and Technology 58 (2016) 482–489

Contents lists available at ScienceDirect

Aerospace Science and Technology

www.elsevier.com/locate/aescte

Optimization of an orbital long-duration rendezvous mission

Jin Zhang *, Guo-jin Tang, Ya-zhong Luo

College of Aerospace Science and Engineering, National University of Defense Technology, Changsha, 410073, China

ARTICLE INFO

Article history:
Received 12 November 2012
Received in revised form 20 August 2016
Accepted 13 September 2016
Available online 19 September 2016

Keywords:
Orbital rendezvous
Long-duration maneuvers
Mixed integer nonlinear programming
Engineering optimization

ABSTRACT

The phasing segment of the rendezvous mission between a cargo spacecraft and a space station usually lasts for several weeks, and actually presents an orbital long-duration problem. In this study, this orbital long-duration problem is formulated as a mixed integer nonlinear programming (MINLP) problem in which the maneuver revolution numbers (integers), maneuver arguments of latitude and impulse magnitude are used as design variables at the same time. A hybrid approach is then proposed to solve this MINLP problem. First, a linear dynamics model considering the J_2 term of the Earth non-spherical gravity is employed to formulate an approximate phasing problem, which is optimized using a genetic algorithm. Second, a shooting iteration process considering the coupling effect between the in-plane and out-of-plane maneuvers is proposed to improve the approximate solution to satisfy the terminal conditions of the high-precision problem. The proposed approach is demonstrated for a typical two-week rendezvous phasing mission. The results show that the proposed approach can stably obtain the near optimal high-precision solution by integrating the perturbed trajectory only a few times. Furthermore, a long-duration rendezvous phasing plan is compatible with any initial phase angles that the in-plane velocity increment remains almost unchanged when the initial phase angle changes. However, under the same conditions, the out-of-plane velocity increment has considerable variations. Compared with a two-day rendezvous phasing plan, a two-week plan could have several successive coplanar launch opportunities for the chaser by aiming different terminal revolution numbers.

1. Introduction

A rendezvous and docking (RVD) mission between a cargo spacecraft and a space station, for example, the RVD between an ATV (Automated Transfer Vehicle) or HTV (H-II Transfer Vehicle) and the ISS (International Space Station) [1,2], usually lasts for several weeks. The rendezvous phasing segment consumes most of the time for a RVD mission [3], and then presents an orbital long-duration problem. For this orbital long-duration problem, in addition to impulses (continuous numbers), the maneuver revolution numbers (integers) could be used as design variables, and the continuous and discrete variables are then investigated at the same time. The optimization of a long-duration rendezvous phasing mission thus is a mixed integer nonlinear programming (MINLP) problem.

RVD has been extensively researched, and is still a hot research topic [4–8]. In a classical survey paper on RVD studies, Jezewski [9] reviewed the planning of rendezvous trajectories from both a theoretical research perspective and an operational application perspective. He pointed out that for a long-duration operational rendezvous mission, orbital perturbations must be taken into account, and that simplified relative motion models could be the foundation of rendezvous targeting algorithms. However, only a few studies have focused on orbital long-duration maneuver problems. Labourdette and Baranov [10] studied a long-duration rendezvous problem with a large initial ascending node difference for the mission involving the return of samples from Mars. They employed a near-circular relative motion model based on orbital element differences with the J_2 perturbation, to optimize the propellant cost and to analyze the relation between that cost and the terminal revolution number. Zhang et al. [11] improved Labourdette and Baranov's model, and applied it to the optimization of in-plane maneuvers in a target spacecraft's long-duration phasing mission.

Recently, the MINLP, a powerful but complicated method, has been applied to the solution of space mission planning problems. Several contributions in this area should be noted here. Ross and D'Souza [12] proposed a hybrid optimal control framework for space mission planning and applied it to the optimization of a multi-agent launch system. Luo et al. [13] proposed a hybrid strategy in the optimization of a two-day rendezvous phasing trajectory with maneuver revolution variables. Zhang et al. [14,15] employed a mixed-code genetic algorithm (GA) to optimize a multi-segment

* Corresponding author. Fax: +86 731 8451 2301.
E-mail addresses: zhangjin@nudt.edu.cn, zhangjinxy1983@gmail.com (J. Zhang).

http://dx.doi.org/10.1016/j.ast.2016.09.011
1270-9638/

Nomenclature

a	semi-major axis
e	eccentricity
I_{sp}	specific impulse of thrusters
i	orbital inclination
k	iteration number of times
l	terminal revolution number changed by maneuvers
N_j	revolution number of the jth maneuver
n	mean angular motion rate
T	orbital period
t_f	end time of the rendezvous phasing mission
t_j	burn time of the jth maneuver
u_j	argument of latitude of the jth maneuver
v	orbital velocity
Δa	difference in semi-major axis
Δi	difference in orbital inclination
Δv_{yj}	in-track impulse of the jth maneuver
Δv_{zj}	cross-track impulse of the jth maneuver
$\Delta\Omega$	difference in right ascension of ascending node
$\Delta\theta$	difference in phase angle
$\Delta\xi$	difference in non-singular orbital element ξ
$\Delta\eta$	difference in non-singular orbital element η
Ω	right ascension of ascending node
ξ	non-singular orbital element, equal to $e\cos\omega$
η	non-singular orbital element, equal to $e\sin\omega$
ω	argument of perigee

Superscript

$-$	related to a mean orbital element

Subscripts

c	related to the chaser
j	related to the jth maneuver
r	related to a reference orbital element
t	related to the target spacecraft
y	related to the in-track direction
z	related to the cross-track direction
aim	related to aimed orbital elements
in	related to in-plane parameters
out	related to out-of-plane parameters

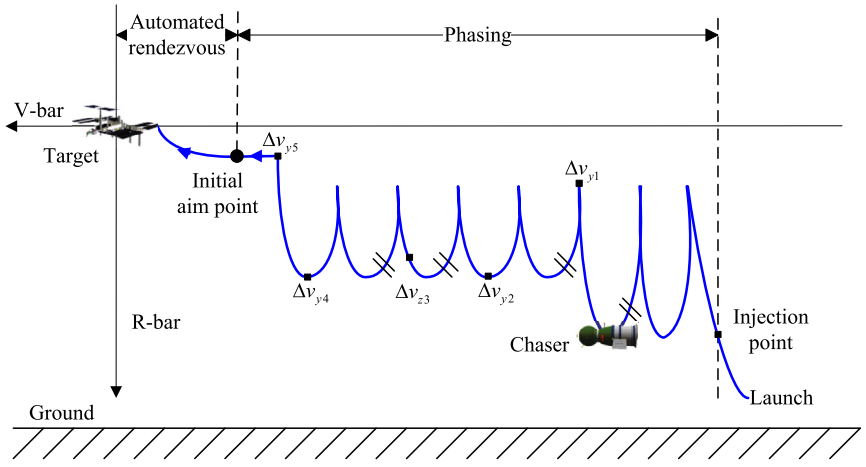

Fig. 1. Rendezvous phasing maneuver plan.

rendezvous mission, and also used the MINLP to solve a low-Earth-orbit (LEO) multi-spacecraft rendezvous problem. MINLP problems, however, remain difficult to solve due to their mixed nature and the potential for multiple local optima [16]. The idea of using maneuver revolution numbers as design variables can also be found in studies on the two-impulse multi-revolution Lambert rendezvous algorithm, in which the two maneuver revolution numbers are enumerated to find the global optimum [17].

The purpose of this paper is to propose a hybrid optimization approach for long-duration rendezvous phasing missions. To avoid having to integrate the long-duration trajectory many times, the approach first presents an approximate optimization problem, which considers the J_2 term of the Earth non-spherical gravity and the coupling effect between in-plane and out-of-plane maneuvers. The solution to the approximate problem is obtained by a GA, and then is improved to a high-precision one by a few iterations.

As mentioned above, reference [11] has employed the MINLP to solve a long-duration in-plane phasing mission of the target spacecraft. Relative to that study, this paper is actually an improvement. First, an out-of-plane maneuver is involved in this paper, which makes the problem more difficult to solve. Second, the coupling effect between the in-plane and out-of-plane maneuvers could bring difficulties to the convergence of the iteration to obtain high-precision solution, and these difficulties will be tackled in the iteration process of this paper.

2. Rendezvous phasing optimization problem

As shown in Fig. 1, the chaser, i.e. the cargo spacecraft, executes several maneuvers to acquire the initial aim point at the end of the rendezvous phasing segment, and the maneuver plan is given as follows.

The first maneuver Δv_{y1}, along the in-track direction, is executed at the apogee to adjust the altitude of the perigee.

The second maneuver Δv_{y2}, along the in-track direction, is executed at the perigee to adjust the altitude of the apogee.

The third maneuver Δv_{z3}, along the cross-track direction, is executed at the argument of latitude u_3 to adjust the orbital inclination and the right ascension of ascending node (RAAN) at the same time.

The fourth maneuver Δv_{y4}, along the in-track direction, is executed at the argument of latitude u_4 (near the perigee) to adjust the apogee altitude to the altitude of the initial aim point.

The fifth maneuver Δv_{y5}, along the in-track direction, is executed at the argument of latitude u_5 (near the apogee) to reduce the eccentricity.

Let t_j and N_j $(j = 1, \ldots, 5)$ be the burn time and revolution number of the jth maneuver respectively, u_1 and u_2 be the arguments of latitude of the first and the second maneuver, and t_0 and t_f be the initial and the end time of the rendezvous phasing segment respectively.

The maneuver plan presented above is similar to the rendezvous phasing maneuver plans of the space shuttle, ATV, HTV and the Shenzhou spacecraft [1–3,18]. The major difference between the rendezvous phasing plans of the manned and unmanned spacecraft is the mission duration. Manned spacecraft needs to consume water, food, and oxygen, and prefers a short rendezvous phasing plan, but unmanned spacecraft allows the use of a relative long rendezvous phasing plan and benefits from available time windows.

The design variables include each maneuver's revolution number, argument of latitude, and impulse magnitude:

$$\mathbf{x} = (N_1, N_2, N_3, N_4, N_5, u_3, u_4, u_5, \Delta v_{y1}, \Delta v_{y2}, \Delta v_{z3}, \Delta v_{y4}, \Delta v_{y5})^T \tag{1}$$

where the locations of the first and the second maneuver are fixed at the apogee and perigee respectively and therefore are not used as design variables.

The objective is to minimize the total velocity increment:

$$\min \Delta v_{total} = \sum_{j=1}^{2} |\Delta v_{yj}| + |\Delta v_{z3}| + \sum_{j=4}^{5} |\Delta v_{yj}| \tag{2}$$

The terminal conditions of the rendezvous phasing segment, i.e. the state of the initial aim point, are constrained by the requirements of the automated rendezvous segment. First, the chaser should be coplanar with the target, which can be expressed by the requirements on the inclination and RAAN:

$$i_c(t_f) - i_t(t_f) = 0 \tag{3}$$

$$\Omega_c(t_f) - \Omega_t(t_f) = 0 \tag{4}$$

where the subscripts "c" and "t" denote the chaser and the target respectively.

Second, at the initial aim point, the chaser should run on a near-circular orbit, which can be expressed as the requirement on the mean eccentricity:

$$\bar{e}_c(t_f) < \varepsilon_e \tag{5}$$

where the superscript "¯" denotes a mean orbital element which is obtained by subtracting the first-order short-period term from an osculating orbital element [19], ε_e is the allowable upper limit of eccentricity.

Third, at the initial aim point, the chaser should run below the target and tens of kilometers away from the target, and these requirements on the orbital altitude difference and the distance between the two spacecraft can be expressed as the constraints on the mean semi-major axis and the argument of latitude:

$$\bar{a}_c(t_f) - \bar{a}_t(t_f) = \Delta \bar{a}_{aim} \tag{6}$$

$$u_c(t_f) - u_t(t_f) = \Delta u_{aim} \tag{7}$$

where $\Delta \bar{a}_{aim}$ and Δu_{aim} are the aimed semi-major axis difference and the aimed argument of latitude difference between the two spacecraft respectively.

The search space of each maneuver's revolution number is limited by telemetry, tracking, and command (TT&C) conditions:

$$N_{jl} \le N_j \le N_{ju} \quad (j = 1, \ldots, 5) \tag{8}$$

where N_{il} and N_{iu} are the lower and upper bounds of the jth maneuver's revolution number respectively.

3. Optimization strategy

In operational applications, the trajectory of a spacecraft is usually calculated by means of high-precision numerical integration. Due to the long phasing duration, it is quite computation-intensive to integrate the trajectory many times. To obtain a good solution at a lower computation cost, an approximate rendezvous phasing model is developed and then optimized using a GA. Finally, a shooting iteration process, which considers the coupling effect between the in-plane and out-of-plane maneuvers, is used to improve the solution to the approximate problem to satisfy the high-precision numerical integration trajectory.

3.1. Approximate optimization problem

For a LEO rendezvous problem, the non-spherical gravity and atmospheric drag are the main perturbations. The non-spherical gravity causes the drift of the ascending node and perigee. Here, a linear dynamics model considering the J_2 term of the non-spherical gravity is employed to approximate the rendezvous maneuver process.

The state variable used to express orbital differences between the chaser and the target is

$$\mathbf{X} = (\Delta a/a_r, \Delta\theta, \Delta\xi, \Delta\eta, \Delta i, \Delta\Omega)^T \tag{9}$$

where the subscript "r" denotes the reference orbit, a_r is the reference semi-major axis, Δa is the difference in semi-major axis, $\Delta\theta$ is the difference in argument of latitude, Δi is the difference in orbital inclination, $\Delta\Omega$ is the difference in RAAN, $\Delta\xi$ and $\Delta\eta$ are the differences in the eccentricity vector $(\xi, \eta)^T = (e\cos\omega, e\sin\omega)^T$, and ω is the argument of perigee.

Using first order approximations, the state transitions of orbital element differences under the J_2 perturbation are given by [15]

$$\begin{cases} \Delta a = \Delta a_0 \\ \Delta\theta = \Delta\theta_0 - \left[\dfrac{3}{2} n_r \dfrac{\Delta a_0}{a_r} + \dfrac{7}{2}\dfrac{\Delta a_0}{a_r} C\left(3 - 4\sin^2 i_r\right)\right]\Delta t \\ \qquad\quad - 4C\sin(2i_r)\Delta i_0 \Delta t \\ \Delta\xi = \Delta\xi_0 \cos(\dot{\omega}_{J_2}\Delta t) - \Delta\eta_0 \sin(\dot{\omega}_{J_2}\Delta t) \\ \Delta\eta = \Delta\xi_0 \sin(\dot{\omega}_{J_2}\Delta t) + \Delta\eta_0 \cos(\dot{\omega}_{J_2}\Delta t) \\ \Delta i = \Delta i_0 \\ \Delta\Omega = \Delta\Omega_0 + \left(\dfrac{7}{2}\dfrac{\Delta a_0}{a_r}\cos i_r + \sin i_r \Delta i_0\right) C\Delta t \end{cases} \tag{10}$$

where the subscript "0" denotes the initial state, Δt is the orbital transfer time, μ is the geocentric gravitation constant, a_e is the mean equatorial radius of the Earth, $n_r = \sqrt{\mu/a_r^3}$ is the mean angular motion rate, $C = \frac{3J_2 a_e^2}{2}\sqrt{\mu} a_r^{-\frac{7}{2}}$, and $\dot{\omega}_{J_2} = C(2 - \frac{5}{2}\sin^2 i_r)$ is the drift rate of perigee.

Based on Eq. (10) and the Gauss's form of variational equations [19], the effects of maneuver impulses on the orbital element differences can be expressed as [15]

$$\begin{cases} \dfrac{\Delta a}{a_r} = 2\dfrac{\Delta v_y}{v_r} \\ \Delta\theta = -\left[3n_r + 7C\left(3-4\sin^2 i_r\right)\right]\Delta t\dfrac{\Delta v_y}{v_r} \\ \qquad -4C\sin(2i_r)\cos u\,\Delta t\dfrac{\Delta v_z}{v_r} \\ \Delta\xi = \sin(u+\dot\omega_{J_2}\Delta t)\dfrac{\Delta v_x}{v_r} + 2\cos(u+\dot\omega_{J_2}\Delta t)\dfrac{\Delta v_y}{v_r} \\ \Delta\eta = -\cos(u+\dot\omega_{J_2}\Delta t)\dfrac{\Delta v_x}{v_r} + 2\sin(u+\dot\omega_{J_2}\Delta t)\dfrac{\Delta v_y}{v_r} \\ \Delta i = \cos u\dfrac{\Delta v_z}{v_r} \\ \Delta\Omega = 7C\cos i_r\Delta t\dfrac{\Delta v_y}{v_r} + \left(\dfrac{\sin u}{\sin i_r} + C\sin i_r\cos u\Delta t\right)\dfrac{\Delta v_z}{v_r} \end{cases} \tag{11}$$

The design variables of the approximate problem are chosen as

$$\mathbf{x}' = (\Delta N_1, \Delta N_2, \Delta N_3, \Delta N_4, \Delta N_5, u_4, u_5, l)^T \tag{12}$$

Let N_f be the terminal revolution number of the chaser, $\Delta N_j = N_f - N_j \approx \frac{t_f - t_j}{T_r}$ be the revolution number difference between the jth maneuver and the initial aim point, where $T_r = 2\pi\sqrt{a_r^3/\mu}$. Based on Eq. (11), the in-plane maneuvers can be expressed as explicit functions of the design variables and terminal in-plane deviations:

$$(\Delta v_{t1}, \Delta v_{t2}, \Delta v_{t4}, \Delta v_{t5})^T = -[\mathbf{y}_1, \mathbf{y}_2, \mathbf{y}_4, \mathbf{y}_5]^{-1}\Delta\mathbf{X}_{in}v_r \tag{13}$$

where

$$\mathbf{y}_j = \begin{bmatrix} 2 \\ [-3n_r - 7C(3-4\sin^2 i_r)]T_r\Delta N_j \\ 2\cos(u_j + \dot\omega_{J_2}T_r\Delta N_j) \\ 2\sin(u_j + \dot\omega_{J_2}T_r\Delta N_j) \end{bmatrix} \quad (j = 1, 2, 4, 5),$$

$$v_r = \sqrt{\frac{\mu}{a_r}},$$

$\Delta\mathbf{X}_{in} = (\delta a/a_r, \delta\theta - 2l\pi, \delta\xi, \delta\eta)^T$ denote the terminal in-plane deviations, and l is the difference between the chaser's terminal number of revolutions in the case of the trajectory with maneuver and in the case of a purely coasting trajectory.

The effect of in-track maneuvers on the terminal RAAN is [15]

$$\Delta\Omega_{in} = 7C\cos i_r\frac{T_r}{v_r}\left(\sum_{j=1}^{2}\Delta N_j\Delta v_{yj} + \sum_{j=4}^{5}\Delta N_j\Delta v_{yj}\right) \tag{14}$$

The out-of-plane maneuver and $\Delta\Omega_{in}$ are both used to adjust the out-of-plane deviations [15]:

$$\begin{pmatrix} 0 \\ \Delta\Omega_{in} \end{pmatrix} + \begin{bmatrix} \cos u_3 \\ \sin u_3/\sin i_r + C\sin i_r\cos u_3 T_r\Delta N_3 \end{bmatrix}\frac{\Delta v_{z3}}{v_r} = -\Delta\mathbf{X}_{out} \tag{15}$$

where $\Delta\mathbf{X}_{out} = (\delta i, \delta\Omega)^T$ are the terminal out-of-plane deviations.

When $\delta i = 0$, the solution to Eq. (15) is

$$\begin{cases} u_3 = 90^\circ \\ \Delta v_{z3} = -(\delta\Omega + \Delta\Omega_{in})\sin i_r v_r \end{cases} \quad \text{or} \quad \begin{cases} u_3 = 270^\circ \\ \Delta v_{z3} = (\delta\Omega + \Delta\Omega_{in})\sin i_r v_r \end{cases} \quad (\delta i = 0) \tag{16a}$$

When $\delta i \neq 0$, the solution to Eq. (15) is

$$\begin{cases} u_3 = \arctan\left[\sin i_r\left(\dfrac{\delta\Omega + \Delta\Omega_{in}}{\delta i} - C_r\sin i_r T_r\Delta N_3\right)\right] \\ \Delta v_{z3} = \dfrac{-\delta i}{\cos u_3}v_r \end{cases} \quad (\delta i \neq 0) \tag{16b}$$

where the quadrant of u_3 could be determined according to its allowable search space.

A hybrid-encoding GA is employed to optimize the approximate problem presented above [15,20]. The design variable vector $\mathbf{x}'$ is directly used as the chromosome. The arithmetical crossover and uniform mutation operators are applied to all genes to diversify the population, and a tournament selection scheme is used to retain good individuals during the evolution. An elitist strategy is employed during the algorithm's selection phase, which can help prevent the loss of good solutions once they have been found. After the crossover and mutation operations, the genes corresponding to integer variables are rounded off to the nearest integers. More applications of GAs to orbital design can be found in references [21–23].

Some relative dynamics models in satellite formation field have considered both the J2 perturbation and the differential drag [24–26], but these models need the assumption of a small relative distance which is not guaranteed in the rendezvous phasing segment. For the rendezvous phasing segment, relative models considering both the J2 perturbation and the differential drag while keeping the additivity of linear models are not available now. Therefore, only the J2 perturbation is considered in the approximate model. One application for the usage of drag for orbital control can be found in reference [22].

3.2. Precise solution using iteration

Reference [11] employed a shooting iteration to improve an approximate solution to a high-precision one. Here, based on the iteration process in reference [11], a shooting iteration considering the coupling effect between the in-plane and out-of-plane maneuvers is proposed. The basic iteration steps are given as follows:

Step 1: Integrate the trajectory of the target spacecraft from t_0 to t_f and calculate its mean terminal state. Based on Eqs. (3)–(7), calculate the aimed mean terminal state of the chaser, and set the iteration number $k = 0$.

Step 2: Only considering a part of the atmospheric drag effect, e.g. "a quarter", integrate the trajectory of the chaser from t_0 to t_f without maneuvers, and then calculate the miss-distances $\delta\mathbf{X}_{in,0} = (\delta a_0/a_r, \delta\theta_0, \delta\xi_0, \delta\eta_0)^T$ and $\delta\mathbf{X}_{out,0} = (\delta i_0, \delta\Omega_0)^T$.

The perigee of the chaser just after injection is very low that the altitude decay effect of the atmospheric drag on the purely coasting trajectory is much larger than the trajectory with maneuvers. Moreover, the altitude decay effect is not considered in the approximate problem. In consequence, only a part of the atmospheric drag effect is considered in Step 2, which could prevent the initial guess from being too far away from the final solution. The value "a quarter" is not necessarily fixed, and it could be changed to "one half", "one third", or "one fifth", which only affects the number of iteration times when the iteration converges to increase or decrease one or two. The usage of part of atmospheric drag for the purely coasting chaser's trajectory is mainly to prevent the trajectory to decay too much.

Step 3: Assign the values of the orbital deviations used to calculate maneuver impulses: $\Delta\mathbf{X}'_{in,k} = \delta\mathbf{X}_{in0}$, $\Delta\mathbf{X}_{out,k} = \delta\mathbf{X}_{out,0}$, and $\Delta\Omega'_{in,k} = \delta\Omega_{in,0} = 0$.

Step 4: Optimize the approximate problem using the GA: for a group values of design variables given by GA, $\Delta\mathbf{X}_{in,k} =$

$\Delta\mathbf{X}'_{in,k} + (0, -2l\pi, 0, 0)^T$, and calculate $(\Delta v_{t1}, \Delta v_{t2}, \Delta v_{t4}, \Delta v_{t5})^T$ using Eq. (12) based on $\Delta\mathbf{X}_{in,k}$; calculate $\Delta\Omega_{in,k}$ using Eq. (13), update it as $\Delta\Omega_{in,k} = \Delta\Omega_{in,k} - \Delta\Omega'_{in,k}$, and then calculate u_3 and Δv_{z3} using Eq. (15).

Step 5: Integrate the trajectory of the chaser using the maneuver data obtained in Step 4 and calculate the terminal miss-distances $\delta\mathbf{X}_{in,k} = (\delta a_k/a_r, \delta\theta_k, \delta\xi_k, \delta\eta_k)^T$ and $\delta\mathbf{X}_{out,k} = (\delta i_k, \delta\Omega_k)^T$.

Step 6: If $\delta\mathbf{X}_{in,k}$ and $\delta\mathbf{X}_{out,k}$ are both in allowable upper limits, stop the iteration and use the solution to the approximate problem as the solution to the original problem; otherwise, go to Step 7.

Step 7: If $k < 3$ or k is an even number, $\Delta\mathbf{X}'_{in,k} = \Delta\mathbf{X}'_{in,k} + \delta\mathbf{X}_{in,k}$; if $k < 3$ or k is an odd number, $\Delta\mathbf{X}_{out,k} = \Delta\mathbf{X}_{out,k} + \delta\mathbf{X}_{out,k} + [0, \Delta\Omega_{in,k}]^T$ and calculate $\Delta\Omega'_{in,k}$ using Eq. (13). $k = k + 1$, return to Step 4.

In Step 7, for the first three iterations, the in-plane and out-of-plane deviations used in the approximate problem are updated simultaneously because $\Delta\Omega_{in,k}$, the effect of in-plane maneuvers on RAAN, takes an important part in the RAAN deviation to be adjusted and it changes a lot during these iterations. As the iteration process runs, $\Delta\Omega_{in,k}$ does not change a lot any more. However, the out-of-plane maneuver affects the in-plane movement a little and this effect is not considered in the approximate problem. After the first three iterations, if the in-plane and out-of-plane deviations used in the approximate problem were still updated simultaneously, the approximate solution can only approach the high-precision solution but cannot satisfy the terminal constraints precisely due to the coupling effect. That is why the in-plane and out-of-plane deviations used in the approximate problem are updated separately after the third iteration. The parameter "three" can be set according to the experience of operators.

4. Results

The proposed approach is demonstrated for a practical fourteen-day (two-week) rendezvous phasing mission. Some numerical experiments are then performed to analyze the properties of long-duration rendezvous phasing missions.

4.1. Problem configuration

The initial time is $t_0 = 0$ s, its corresponding Gregorian universal coordinated time (UTCG) in the calculation is set as 21 June 2010 00:00:00.0, and the end time is $t_f = 1209600$ s (14 days). The initial states of the target spacecraft and the chaser in the form of classical osculating orbital elements (semi-major axis, eccentricity, inclination, RAAN, argument of perigee, true anomaly) are given respectively by

$$\mathbf{E}_t(t_0) = \left(6720.14\,\text{km},\ 1.0\text{e}{-5},\ 42^\circ,\ 169.2^\circ,\ 100^\circ,\ 145^\circ\right),$$

$$\mathbf{E}_c(t_0) = \left(6638.14\,\text{km},\ 0.009039,\ 42.05^\circ,\ 171.6^\circ,\ 120^\circ,\ 1^\circ\right).$$

The orbital perturbations considered include both the non-spherical gravity and the atmospheric drag. The spherical harmonic gravity model used is the Joint Gravity Model 3 (JGM3) [27], and both the degree and order are set to 10. The atmospheric density model used is the NRLMSISE-00 (Naval Research Laboratory Mass Spectrometer and Incoherent Scatter Radar Exosphere 2000) model [28]. The other force model parameters for numerical trajectory integration are provided in Table 1. The Runge–Kutta–Fehlberg 7th order integrator with the 8th order error control [29] is used with an integral step of 60 s. The Earth's mean radius is $a_e = 6378.137$ km. The initial revolution numbers for the two spacecraft are both 1, and the terminal revolution number for the target, obtained by numerical integration, is 222. The reference semi-major axis is chosen as the mean value of the target's and the chaser's initial semi-major axis, and the other reference orbital elements are the same as the target orbit.

Table 1
Spacecraft's force model parameters.

Item	Value
Mass of the target	10000 kg
Mass of the chaser	8000 kg
Drag area of the target	30 m^2
Drag area of the chaser	20 m^2
Drag coefficient	2.2
Sea-level standard acceleration of gravity	9.80665 m/s^2
Specific impulse (I_{sp}) of thrusters	305.91486 s
Daily F10.7 index	150
Average F10.7 index	150
Geomagnetic flux index (k_p)	4

Table 2
GA parameters.

Item	Value
Population size	500
Maximum number of generations	100
Scale of tournament selection	3
Probability of crossover	0.5
Probability of mutation	0.3

The lower and upper bounds on revolution number variables are [3, 15], [17, 30], [90, 105], [180, 195] and [197, 210], such that the first and second maneuvers are executed near the initial part of the mission, the fourth and the fifth maneuvers are executed near the terminal part of the mission, and the third is executed at the middle part of the mission. $\Delta\bar{a}_{aim} = -15$ km and $\Delta u_{aim} = -0.445^\circ$. The convergence criterions for the terminal mean semi-major axis, argument of latitude and mean eccentricity are $\varepsilon_a = 0.2$ km, $\varepsilon_u = 0.001^\circ$ and $\varepsilon_e = 1.0\text{e}{-4}$ respectively, and the convergence criterions for the terminal inclination and RAAN are $\varepsilon_i = 0.001^\circ$ and $\varepsilon_\Omega = 0.001^\circ$ respectively. The parameters for the GA employed are listed in Table 2. Moreover, "a part" of atmospheric drag used in Step 2 of the iteration is "a quarter" for this numerical example.

4.2. Optimal solution

According to the data provided above, the rendezvous phasing problem is successfully solved using the proposed optimization strategy. The total velocity increment obtained is 72.517 m/s, and the corresponding propellant consumption is 191.061 kg. The maneuver revolution numbers, arguments of latitude and impulses are provided in Table 3, and the terminal miss-distance errors during the iteration process are presented in Table 4. The time histories of the phase angle and the chaser's mean semi-major axis are shown in Fig. 2 and Fig. 3 respectively.

From Table 4, it can be obtained that the terminal miss-distances decrease gradually and stably as k increases. When $k = 9$, the miss-distances satisfy the convergence criterions and therefore the iteration stops. The terminal revolution number of the chaser is adjusted from 226 (non-maneuver trajectory) to 224, i.e. $l = -2$.

In Table 3, the in-track impulses obtained are all positive, and this confirms the near optimality of the in-plane transfer because all in-track impulses are used to raise the altitude of a near-circular orbit. When l is fixed at -1, the minimum velocity increment obtained is 102.008 m/s; when l is fixed at -3, the minimum velocity obtained is 152.831 m/s. Both of them are greater than the velocity increment obtained by the proposed approach, which partly indicates the effectiveness of the optimization process.

Table 3
Maneuver data.

Maneuver sequence	1	2	3	4	5
Revolution number	6	23	90	190	207
Argument of latitude (°)	304.82369	125.44699	257.41309	55.31065	305.42823
Impulse (m/s)	18.43831	2.04364	30.21971	14.53279	7.28285

Table 4
Terminal miss-distances during the iteration.

k	$\delta\bar{a}$ (km)	$\bar{e}$	$\delta\theta$ (°)	δi (°)	$\delta\Omega$ (°)	N_f
0	−70.658	0.0073072	−0.66434	0.04899	−1.39241	226
1	−3.241	0.0005287	22.06829	−0.00034	−0.02062	224
2	0.378	0.0000825	−3.82816	−0.00010	0.01060	224
3	−0.037	0.0000852	0.36501	−0.00009	0.00956	224
4	−0.032	0.0000876	0.31488	0.00003	0.00018	224
5	0.003	0.0000872	−0.03036	0.00003	0.00027	224
6	0.003	0.0000873	−0.03160	−4.56e−6	1.50e−6	224
7	0.003	0.0000863	0.00420	0.00006	0.00002	224
8	0.003	0.0000863	0.00423	0.00006	0.00003	224
9	0.003	0.0000858	−0.00048	0.00005	0.00003	224

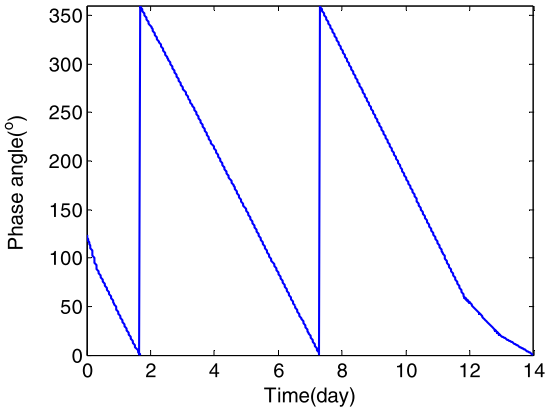

Fig. 2. Time history of the phase angle.

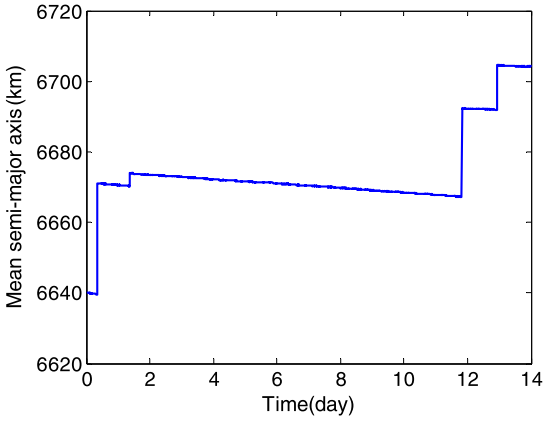

Fig. 3. Time history of the chaser's mean semi-major axis.

4.3. Property analysis

To analyze to the effect of the initial phase angle on the velocity increment, a group of phase angle variations $\Delta u_{t0} \in [-180°,\ 180°]$ are added to the target's initial argument of latitude, while the other initial mean orbital elements remain unchanged in the calculation. The values of the total velocity increment, out-of-plane impulse and in-plane velocity increment for the group of Δu_{t0} are all shown in Fig. 4, where $\Delta v_{in-plane} = \Delta v_{total} - |\Delta v_z|$. A comparative numerical trial is made and shown in Fig. 5, where the maneuver revolution numbers are 3, 6, 15, 24 and 28, the time of flight is 172800 s (two days), the target's initial RAAN is 169.2°, and the other problem configurations are the same as the two-week mission. The mission duration of "two days" was used in the rendezvous plan of the Space shuttle, the Soyuz and Progress spacecraft before 2012, and the Shenzhou spacecraft, and therefore is used as the typical relative short rendezvous time length for comparison [13]. It should be noted that the relative short two-day mission is still much longer than the six-hour short rendezvous profile of Soyuz and Progress spacecraft after 2012 [30,31].

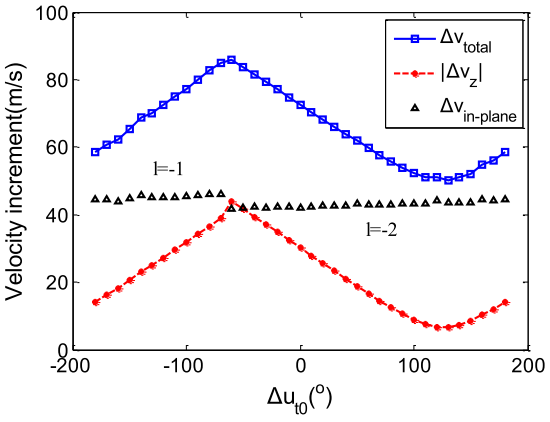

Fig. 4. Velocity increment vs. difference in the target's initial argument of latitude (two-week mission).

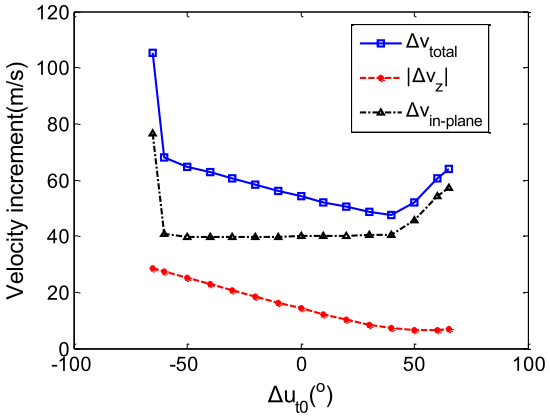

Fig. 5. Velocity increment vs. difference in the target's initial argument of latitude (two-day mission).

From Fig. 4, it can be found that the variation magnitude of the total velocity increment is almost the same as the variation of the out-of-plane impulse. Therefore, from the point view of the in-plane transfer, a long-duration phasing plan is compatible with any initial phase angles that the in-plane velocity increment remains almost unchanged. However, a two-day phasing plan does not has this property that when $|\Delta u_{t0}| > 50°$, obvious in-plane velocity increments have appeared in Fig. 5. From the point view of the out-of-plane adjustment, the initial phase angle, an in-plane factor, has a considerable effect on the out-of-plane velocity increment through the effect of in-plane maneuvers on the drift of RAAN. This confirms the necessity of considering Eq. (13) in the approximate problem.

To analyze to the effect of the initial RAAN on the velocity increment, a group of RAAN variations $\Delta\Omega_{c0} \in [-1.5°,\ 1.0°]$ are

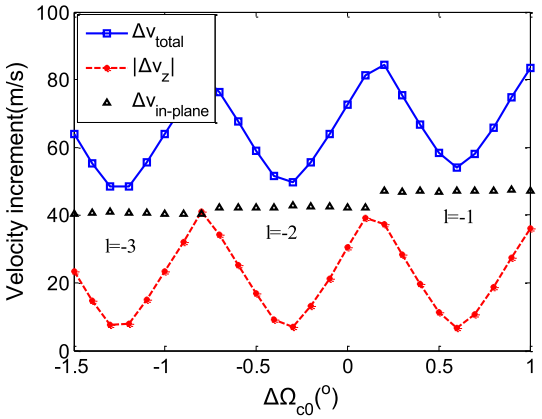

Fig. 6. Velocity increment vs. difference in the chaser's initial RAAN (two-week mission).

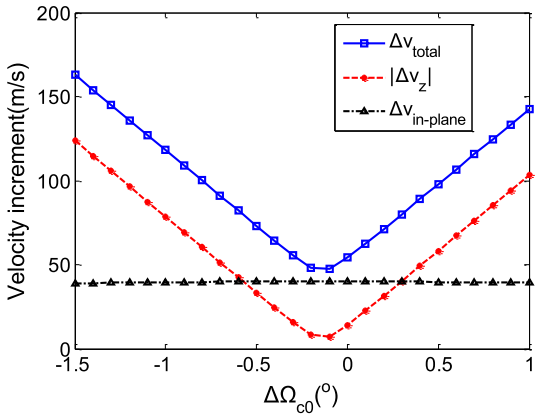

Fig. 7. Velocity increment vs. difference in the chaser's initial RAAN (two-day mission).

added to the chaser's initial RAAN, while the other initial mean orbital elements remain unchanged in the calculation. The values of the total velocity increment, in-plane velocity increment and out-of-plane impulse are all shown in Fig. 6. A comparative numerical trial with a two-day rendezvous phasing mission is made again and shown in Fig. 7, where the problem configuration corresponding to $\Delta\Omega_{c0} = 0$ is the same as that of Fig. 5.

From Fig. 6, it can be found that there are three local minimums as the $\Delta\Omega_{c0}$ varies from $-1.5°$ to $1.0°$, and each minimum corresponds to a different revolution correction number l. In contrast, for the two-day mission in Fig. 7, there is only one local minimum. Thus, by aiming different terminal revolution numbers (i.e. different values of l), a long-duration rendezvous phasing plan can be compatible with a much wider initial RAAN interval than a typical two-day phasing plan. Furthermore, one local minimum point actually corresponds to one coplanar launch opportunity of the chaser, and then a long-duration rendezvous phasing plan could have several successive launch opportunities. This will benefit the practical operation of a rendezvous mission.

5. Conclusion

This paper has presented a hybrid optimization approach for long-duration rendezvous phasing missions and then has demonstrated it for a typical two-week rendezvous phasing mission. The results show that the proposed approach can stably obtain the near optimal high-precision solution by integrating the perturbed trajectory only a few times.

A long-duration rendezvous phasing plan is compatible with any initial phase angles that the in-plane velocity increment remains almost unchanged when the initial phase angle changes. However, under the same conditions, the out-of-plane velocity increment has considerable variations, which is caused by the coupling effect between in-plane and out-of-plane maneuvers.

For a typical two-day rendezvous phasing plan, or plans with shorter mission duration, the total velocity increment has only one local minimum when the initial right ascension of ascending node (RAAN) of the chaser changes, and that local minimum corresponds to a quasi-coplanar launch opportunity of the chaser. However, for a long-duration rendezvous phasing plan, such as the plan with two-week mission duration, the total velocity increment has multiple local minimums as the initial RAAN of the chaser changes, and different local minimums correspond to different terminal revolution numbers. By aiming different terminal revolution numbers, a two-week plan could have more successive quasi-coplanar launch opportunities for the chaser (cargo spacecraft) than a two-day rendezvous phasing plan.

Conflict of interest statement

The authors declared that they have no conflicts of interest to this work.

Acknowledgements

This work was partly supported by the National Natural Science Foundation of China (No. 11402295) and the Science Project of the National University of Defense Technology (No. JC14-01-05).

References

[1] ESA, ATV-1: Jules Verne, http://www.esa.int/esaMI/ATV/SEM92X6K56G_0.html. Accessed July 2012.
[2] K. Wada, S. Kobayashi, N. Motoyama, M. Suzuki, Evaluation and findings of HTV-1 trajectory and the planning operation, IAC-10.C1.6.6, in: 61st International Astronautical Congress, Prague, CZ, 2010.
[3] W. Fehse, Automated Rendezvous and Docking of Spacecraft, Cambridge University Press, Cambridge, 2003.
[4] X.B. Yang, X.B. Cao, A new approach to autonomous rendezvous for spacecraft with limited impulsive thrust: based on switching control strategy, Aerosp. Sci. Technol. 43 (2015) 454–462.
[5] W.M. Feng, D. Zhao, L. Shi, et al., Optimization control for the far-distance rapid cooperative rendezvous of spacecraft with different masses, Aerosp. Sci. Technol. 45 (2015) 449–461.
[6] X. Huang, Y. Yan, Y. Zhou, et al., Output feedback control of Lorentz-augmented spacecraft rendezvous, Aerosp. Sci. Technol. 42 (2015) 241–248.
[7] Y.Z. Luo, G.J. Tang, Rendezvous phasing special-point maneuvers mixed discrete-continuous optimization using simulated annealing, Aerosp. Sci. Technol. 10 (2006) 652–658.
[8] L. Sun, W. Huo, Robust adaptive relative position tracking and attitude synchronization for spacecraft rendezvous, Aerosp. Sci. Technol. 41 (2015) 28–35.
[9] D.J. Jezewski, J.P. Brazzel, E.E. Prust, B.G. Brown, T.A. Mulder, D.B. Wissinger, A survey of rendezvous trajectory planning, Adv. Astronaut. Sci. 76 (1992) 1373–1396.
[10] P. Labourdette, A.A. Baranov, Software for rendezvous between near-circular orbits with large initial ascending node difference, in: Proc. XVI Scientific Lecture on Astronautics, January 24–26, 2001, Moscow, 2001.
[11] J. Zhang, X. Wang, X.B. Ma, Y. Tang, H.B. Huang, Spacecraft long-duration phasing maneuver optimization using hybrid approach, Acta Astronaut. 72 (2012) 132–142.
[12] I.M. Ross, C.N. D'Souza, Hybrid optimal control framework for mission planning, J. Guid. Control Dyn. 28 (4) (2005) 686–697.
[13] Y.Z. Luo, H.Y. Li, G.J. Tang, Hybrid approach to optimize a rendezvous phasing strategy, J. Guid. Control Dyn. 30 (1) (2007) 185–191.
[14] J. Zhang, G.J. Tang, Y.Z. Luo, H.Y. Li, Orbital rendezvous mission planning using mixed integer nonlinear programming, Acta Astronaut. 68 (2011) 1070–1078.
[15] J. Zhang, Y.Z. Luo, G.J. Tang, Hybrid planning for LEO long-duration multi-spacecraft rendezvous mission, Sci. China, Technol. Sci. 55 (1) (2012) 233–243.
[16] V.B. Gantovnik, Z. Gurdal, L.T. Watson, C.M. Anderson-Cook, Genetic algorithm for mixed integer nonlinear programming problems using separate constraint

approximations, AIAA J. 43 (8) (2005) 1844–1849.
[17] H.J. Shen, P. Tsiotras, Optimal two-impulse rendezvous using multiple-revolution Lambert solutions, J. Guid. Control Dyn. 26 (1) (2003) 50–61.
[18] B.N. Zhang, X.B. Ma, W. Zheng, et al., Design and implementation of China's manned rendezvous and docking technology, Sci. Sin. (Technol.) 44 (1) (2014) 1–11 (in Chinese).
[19] D.A. Vallado, Fundamentals of Astrodynamics and Applications, second ed., Microscosm Press, Torrance, California, 2001.
[20] K. Deep, K.P. Singh, M.L. Kansal, C. Mohan, A real coded genetic algorithm for solving integer and mixed integer optimization problems, Appl. Math. Comput. 212 (2009) 505–518.
[21] O. Omarabdelkhalik, D. Mortari, Orbit design for ground surveillance using genetic algorithms, J. Guid. Control Dyn. 29 (5) (2006) 1231–1235.
[22] G.B. Palmerini, S. Sgubini, G. Taini, Spacecraft orbit control using air drag, in: 56st International Astronautical Congress, IAC-05.C1.6.10, Fukuoka, Japan, 2005.
[23] G. Taini, L. Amorosi, A. Notarantonio, G.B. Palmerini, Applications of genetic algorithms in mission design, in: IEEE Aerospace Conference, MT, USA, 2005.
[24] K.T. Alfriend, S.R. Vadali, P. Gurfil, et al., Spacecraft Formation Flying: Dynamics, Control, and Navigation, Butterworth–Heinemann, 2009.
[25] M. Sabatini, G.B. Palmerini, Linearized formation-flying dynamics in a perturbed orbital environment, in: IEEE Aerospace Conference, Big Sky, MT, USA, 2008.
[26] L. Cao, A.K. Misra, Linearized J2 and atmospheric drag model for satellite relative motion with small eccentricity, in: Proceedings of the Institution of Mechanical Engineers, Part G, J. Aerosp. Eng. 229 (14) (2015) 2718–2736.
[27] B.D. Tapley, M.M. Watkins, et al., The joint gravity model 3, J. Geophys. Res. 101 (B12) (1996) 28029–28050.
[28] J.M. Picone, A.E. Hedin, D.P. Drob, A.C. Aikin, NRLMSISE-00 empirical model of the atmosphere: statistical comparisons and scientific issues, J. Geophys. Res. 107 (A12) (2002) 1468–1483.
[29] E. Fehlberg, Classical fifth-, sixth-, seventh-, and eighth-order Runge–Kutta formulas with step size control, NASA TR R-287, NASA Technical Report, 1968.
[30] R.F. Murtazin, N. Petrov, Short profile for the human spacecraft Soyuz-TMA rendezvous Mission to the ISS, Acta Astronaut. 77 (2012) 77–82.
[31] R.F. Murtazin, N. Petrov, Usage of pre-flight data in short rendezvous mission of Soyuz-TMA spacecraft, Acta Astronaut. 93 (2014) 71–76.